



**Dual Acting Oximes Designed for Therapeutic  
Decontamination of Reactive Organophosphates via  
Catalytic Inactivation and Acetylcholinesterase Reactivation**

Journal:	<i>RSC Medicinal Chemistry</i>
Manuscript ID	MD-RES-06-2021-000194.R2
Article Type:	Research Article
Date Submitted by the Author:	02-Aug-2021
Complete List of Authors:	Cannon, Jayme; University of Michigan, Michigan Nanotechnology Institute for Medicine and Biological Sciences Tang, Shengzhuang; University of Michigan, Yang, Kelly; University of Michigan, Michigan Nanotechnology Institute for Medicine and Biological Sciences Harrison, Racquel; University of Michigan, Michigan Nanotechnology Institute for Medicine and Biological Sciences Choi, Seok Ki; University of Michigan Medical Center,

## ARTICLE

## Dual Acting Oximes Designed for Therapeutic Decontamination of Reactive Organophosphates via Catalytic Inactivation and Acetylcholinesterase Reactivation

Received 00th January 20xx,  
Accepted 00th January 20xx

DOI: 10.1039/x0xx00000x

Jayme Cannon,<sup>ab</sup> Shengzhuang Tang,<sup>ab</sup> Kelly Yang,<sup>a</sup> Racquel Harrison<sup>a</sup> and Seok Ki Choi<sup>\*ab</sup>

A conventional approach in the therapeutic decontamination of reactive organophosphate (OP) relies on chemical OP degradation by oxime compounds. However, their efficacy is limited due to their lack of activity in the reactivation of acetylcholinesterase (AChE), the primary target of OP. Here, we describe a set of  $\alpha$ -nucleophile oxime derivatives which are newly identified for such dual modes of action. Thus, we prepared a 9-member oxime library, each composed of an OP-reactive oxime core linked to an amine-terminated scaffold, which varied through an *N*-alkyl functionalization. This library was screened by enzyme assays performed with human and electric eel subtypes of OP-inactivated AChE, which led to identifying three oxime leads that displayed significant enhancements in reactivation activity comparable to 2-PAM. They were able to reactivate both enzymes inactivated by three OP types including paraoxon, chlorpyrifos and malaoxon, suggesting their broad spectrum of OP susceptibility. All compounds in the library were able to retain catalytic reactivity in paraoxon inactivation by rates increased up to 5 or 8-fold relative to diacetylmonoxime (DAM) under controlled conditions at pH (8.0, 10.5) and temperature (17, 37 °C). Finally, selected lead compounds displayed superb efficacy in paraoxon decontamination on porcine skin *in vitro*. In summary, we addressed an unmet need in therapeutic OP decontamination by designing and validating a series of congeneric oximes that display dual modes of action.

### Introduction

Reactive organophosphates (OPs) constitute a class of chemical threat agents that pose serious threats to human health.<sup>1,2</sup> They collectively refer to phosphorous-based (thio)esters which span from common pesticides such as parathion and its active metabolite paraoxon (POX) to nerve agents such as sarin (Fig. 1).<sup>3,4</sup> Their high reactivity is ascribed to the electrophilic phosphorous ester which participates in covalent modifications of proteins and enzymes.<sup>3,5,6</sup> Human toxicity induced by OPs results from the inactivation of acetylcholinesterase (AChE) as their primary target.<sup>1,3,5</sup> This occurs within the enzyme catalytic pocket where OP forms a covalent adduct at serine-203 through *O*-phosphorylation.<sup>7</sup> Such enzyme inactivation constitutes a fundamental basis of OP toxicity which involves acetylcholine accumulation and as a consequence, excessive stimulations of acetylcholine receptor at cholinergic nerve systems.<sup>1,3</sup>

Therapeutic agents developed in the treatment of OP intoxication include atropine (acetylcholine receptor blocker)<sup>8,9</sup> and quaternary oximes such as 2-PAM and obidoxime.<sup>3,10,11</sup> Each of these oximes serves as an enzyme reactivator due to its

nucleophilic oxime reactivity that catalyzes the hydrolysis of the *O*-phosphorylated serine to a free serine (Fig. 1B). However, these oximes suffer from certain drawbacks<sup>12</sup> that have stimulated significant efforts towards longer duration of action,<sup>13</sup> improved bioavailability in the central nervous systems<sup>14-16</sup> and the ability for resurrecting OP-aged enzymes.<sup>17</sup>

Another essential approach for OP treatment involves OP inactivation using scavengers such as OP-reactive oxime molecules,<sup>18-21</sup> esterase-based bioscavengers<sup>22,23</sup> and OP-responsive nanomaterials<sup>24</sup> that include copper-chelated bipyridyl polymers,<sup>25</sup> La(catecholate)-functionalized porous polymers,<sup>26</sup> metal-organic frameworks<sup>27,28</sup> and dendrimer nanoreactors.<sup>29,30</sup> Development of these OP scavengers also plays a critical role in the therapeutic decontamination of the OP exposed skin because unless treated, extended OP absorption occurs leading to sustained toxicity.<sup>31</sup> This is illustrated with reactive skin decontamination lotion (RSDL)<sup>18</sup> which is formulated with an active ingredient Dekon 139, the potassium salt of diacetylmonoxime (DAM), at 1.2 M, pH  $\geq$  10.8. This oxime molecule, which exists predominantly as an oximate form under the formulated condition, catalyzes OP inactivation via its nucleophilic attack at the phosphorous atom (Fig. 1B). However, despite importance in OP decontamination, lipophilic oximes are associated with undesired properties that include rapid percutaneous absorption, membrane distribution which is reported to account for skeletal muscle paralysis<sup>32,33</sup> and impaired wound healing.<sup>34</sup> Due to such adverse effects, RSDL<sup>34,35</sup> has been approved for intact skin decontamination only but not for open wounds or mucous membranes. Thus, there

<sup>a</sup> Michigan Nanotechnology Institute for Medicine and Biological Sciences, University of Michigan Medical School, Ann Arbor, Michigan 48109, United States of America. \*E-mail: [skchoi@umich.edu](mailto:skchoi@umich.edu). ORCID: 0000-0001-5633-4817

<sup>b</sup> Department of Internal Medicine, University of Michigan Medical School, Ann Arbor, Michigan 48109, United States of America

† Electronic Supplementary Information (ESI) available: Details for oxime synthesis, copies of mass spectra, <sup>1</sup>H and <sup>13</sup>C NMR spectra, UPLC traces, supplementary figures and tables are provided. See DOI: 10.1039/x0xx00000x

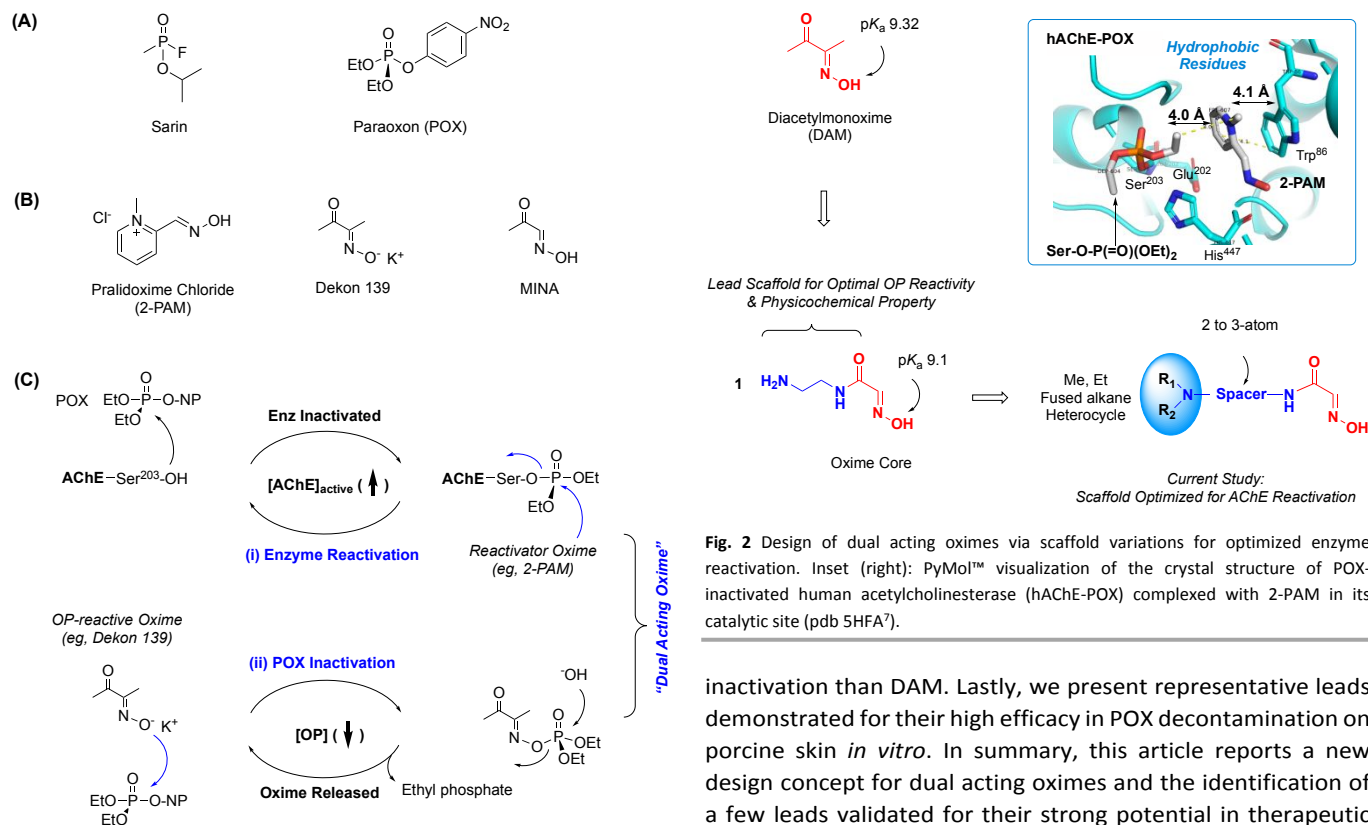


**Fig. 1** (A) Structures of representative reactive organophosphates (OP). (B) Structures of two classes of oxime-based therapeutic agents including 2-PAM, Dekon 139 (potassium salt of diacetylmonoxime) and monoisonitrosoacetone (MINA), each used in the treatment of OP poisoning or topical OP decontamination, respectively. (C) Two therapeutic mechanisms of action conferred by a dual acting oxime as illustrated with 2-PAM as an acetylcholinesterase (AChE) reactivator and Dekon 139 as a catalytic OP inactivator.

remains a significant unmet need for developing more safe and effective OP decontaminants that enable to prevent persistent OP toxicity.

In the present study, we are interested in exploring a multifunctional approach in the development of OP therapeutics in which a single molecule confers dual modes of action: i) enzyme reactivation; ii) OP inactivation. This concept has been previously tested using lipophilic oximes DAM and monoisonitrosoacetone (MINA) with limited success, in part, due to their poor reactivation activity.<sup>36, 37</sup> However, if further optimized, dual activities can be more beneficial than either activity alone.

Here we present an enzyme structure-guided design of a 9-member oxime library, their synthesis and *in vitro* evaluations performed with a focus on such dual actions. Each designed oxime molecule consists of two orthogonal moieties: an OP-reactive core, which remains constant, linked to an amine-terminated scaffold which serves a variable domain for improved ability in enzyme reactivation. We present biochemical evidence for the occurrence of enzyme reactivation as good as 2-PAM against several types of OP-inactivated AChE. We describe a kinetic assay for POX hydrolysis and present rate constants of these oximes that are indicative of faster

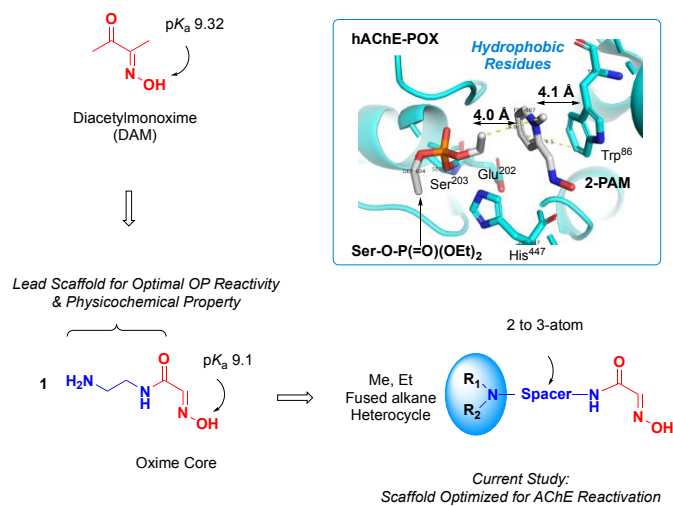


**Fig. 2** Design of dual acting oximes via scaffold variations for optimized enzyme reactivation. Inset (right): PyMol™ visualization of the crystal structure of POX-inactivated human acetylcholinesterase (hAChE-POX) complexed with 2-PAM in its catalytic site (pdb 5HFA<sup>7</sup>).

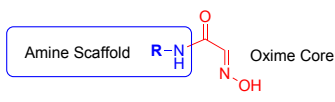
inactivation than DAM. Lastly, we present representative leads demonstrated for their high efficacy in POX decontamination on porcine skin *in vitro*. In summary, this article reports a new design concept for dual acting oximes and the identification of a few leads validated for their strong potential in therapeutic OP decontamination.

## Results and discussion

### 1. Design of Dual Acting Oximes

In our recent works,<sup>19, 20</sup> we validated hydrophilic scaffolds of oxime and hydroxamic acid-based  $\alpha$ -nucleophiles<sup>21</sup> as the chemical scavengers of OP. These led to the identification of promising leads including **1** (Fig. 2), an amine scaffold tethered to an oxime reactive core that belongs in a 2-hydroxyiminoacetamide series.<sup>20</sup> In the current approach, oxime **1** served as a lead structure due to its superb OP reactivity enabled by its nucleophilic oxime ( $pK_a = 9.1$ ).<sup>20</sup> Its amine-terminated scaffold also offers a good hydrophilicity ( $clogP = -1.488$ ), which can be beneficial for preventing an adverse percutaneous absorption associated with lipophilic DAM. On the other hand, its activity for enzyme reactivation occurs only at a suboptimal level compared to 2-PAM.<sup>20</sup> So, we considered keeping its 2-hydroxyiminoacetamide core to retain OP reactivity but making structural variations in its scaffold domain only by which the ability for enzyme reactivation can be optimized.

Ideas for scaffold variations were developed using the resolved structure of hAChE inactivated by POX<sup>7</sup> which shows the presence of hydrophobic residues within its narrow catalytic pocket (inset, Fig. 2). These include an aromatic indole residue at tryptophan-86 which constitutes a choline binding site through its cation- $\pi$  interaction<sup>38</sup> as well as two non-enzymatic ethoxy residues which are introduced as a result of POX phosphorylation at serine-203. Of particular note is their close proximity to an oxime reactivator (2-PAM) within  $\sim 4$  Å in spatial

**Table 1** Structures and physicochemical properties of oxime compounds 1–9


Entry	Scaffold (R)	clogP <sup>a</sup>	CMR <sup>b</sup>	P <sub>e</sub> × 10 <sup>6</sup> <sup>c</sup>	Rel. P <sub>e</sub>
DAM	-	0.332	2.72	6.0 (±0.20)	1.00
1	H <sub>2</sub> N(CH <sub>2</sub> ) <sub>2</sub> -	-1.49	3.45	1.4 (±0.14)	0.23
2	Me <sub>2</sub> N(CH <sub>2</sub> ) <sub>2</sub> -	-0.590	4.38	2.2 (±0.22)	0.38
3	Me <sub>3</sub> N <sup>+</sup> (CH <sub>2</sub> ) <sub>2</sub> -	-4.56	4.93	1.6 (±0.14)	0.27
4	Et <sub>2</sub> N(CH <sub>2</sub> ) <sub>2</sub> -	0.468	5.31	1.1 (±0.12)	0.18
5	(CH <sub>2</sub> ) <sub>4</sub> N(CH <sub>2</sub> ) <sub>2</sub> -	0.047	5.13	1.1 (±0.08)	0.18
6	Me <sub>2</sub> N(CH <sub>2</sub> ) <sub>3</sub> -	-0.317	4.85	1.8 (±0.16)	0.30
7	Im(C2)-CH <sub>2</sub> -	-2.15	4.35	1.1 (±0.12)	0.19
8	H <sub>2</sub> NCH <sub>2</sub> CH(OH)CH <sub>2</sub> -	-2.31	4.07	0.81 (±0.10)	0.14
9	HOCH <sub>2</sub> CH(OH)CH <sub>2</sub> -	-1.68	3.86	0.61 (±0.10)	0.10

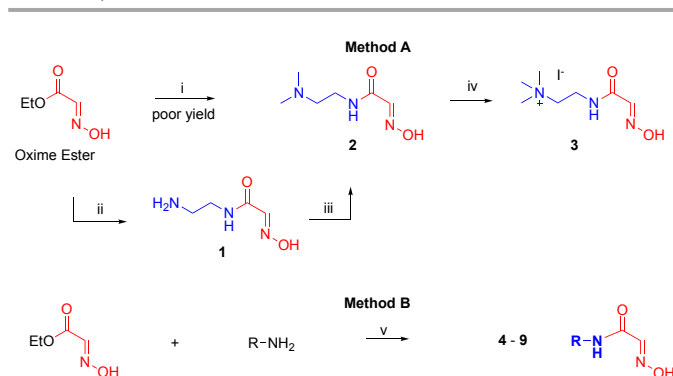
<sup>a</sup> cLogP = log of calculated partition coefficient (*P*) between 1-octanol and water where  $P = [\text{oxime}]_{1\text{-octanol}}/[\text{oxime}]_{\text{water}}$ . <sup>b</sup> CMR = calculated molar refractivity (m<sup>3</sup> mol<sup>-1</sup>). Both calculated using ChemDraw Software (Professional 16.0). <sup>c</sup> Effective permeability coefficient (*P<sub>e</sub>*, cm s<sup>-1</sup>) determined as a mean value at 23 °C in a parallel artificial membrane permeability assay (PAMPA).<sup>39</sup> Each value within parentheses represents a standard deviation (SD) associated with detection wavelengths. Rel. *P<sub>e</sub>* refers to a ratio of *P<sub>e</sub>* (oxime) to *P<sub>e</sub>* (DAM).

distance. Thus, we hypothesized that adding a small hydrophobic motif at the amine terminus of **1** could help create more favourable interactions with those hydrophobic residues and as a consequence, induce a better fit at the phosphorylated site where its oxime core engages in a nucleophilic attack, releasing the serine as its active hydroxyl form.

Based on this strategy, we constructed a focused library of oxime compounds **2–9** as summarized in Table 1. These are variable only at the scaffold domain with the addition of hydrophobic motifs at a two (**2–5**) or three-carbon spacer (**6**). Thus, **2–6** each contains two or three small alkyl moieties such as methyl, ethyl or pyrrolidinyl attached at the amine terminus. A few comparators were also included in the library such as **7** which is terminated with an imidazole heterocycle with a spacing of two atoms apart from its amide nitrogen. We included two hydrophilic comparators **8, 9**, each presenting amine and hydroxyl moieties substituted at the three-carbon spacer. Other than these variations, we were not interested in longer spacers or other alkyl groups which are bulky, branched or lengthy because of potential detrimental effects caused by their steric congestion within the pocket. In summary, we selected a 9-member library, each structurally identical in their reactive core but variable in their scaffolds through hydrophobic augmentation (**2–6**), quaternary *N*-alkylation (**3**) and attachment with a flat heterocycle (**7**) or hydrophilic groups (**8, 9**).

## 2. Synthesis of Dual Acting Oximes

Compounds **1–9** were synthesized according to method A and method B in Scheme 1 using ethyl 2-(hydroxyimino)acetate, an

**Scheme 1** Synthetic methods of oximes 1–9

**Reagents and conditions:** i) *N,N*-Dimethylethylenediamine (3 equiv), EtOH, rt to 45 °C, 2 h (26%); ii) Ethylenediamine, EtOH, rt, 3 h (quantitative); iii) Formaldehyde, EtOH, rt, 30 min; then NaCNBH<sub>3</sub>, 50 °C, 16 h (66%); iv) Methyl iodide, MeOH, 40 °C, 12 h (75%); v) RNH<sub>2</sub> (3 equiv), EtOH, 45 °C, 2 h to 48 h (68% to quantitative). Confer Table 1 for R-NH<sub>2</sub>. rt = room temperature

oxime ester which was prepared from ethyl glyoxylate by treatment with hydroxylamine.<sup>40</sup> All oximes except **3** were prepared in one step through the amidation of the oxime ester (68% to quantitative) by reacting with a series of primary amine (R-NH<sub>2</sub>) as shown in Table 1. However, the synthesis of **2** by this method was less efficient due to its poor yield (26%), and alternatively it was prepared more efficiently in two steps (method A) via *N*-reductive alkylation of **1**. Lastly, **3**, the quaternary ammonium salt, was prepared through *N*-methylation of **2** by treatment with methyl iodide.<sup>41</sup>

All compounds were purified by silica column chromatography and fully characterized for their homogeneity (≥95%) by ultra-performance liquid chromatography (UPLC) analysis and their identity by <sup>1</sup>H and <sup>13</sup>C NMR spectroscopy and high-resolution mass spectrometry (Fig. S1, S2) as described in Electronic Supplementary Information (ESI). These analytical data are supportive of their structural features and consistent with literature data reported elsewhere (**1**,<sup>10, 20</sup> **4**,<sup>10</sup> **5**,<sup>42</sup> **6**<sup>10</sup>). Oximes in this library set remained stable in phosphate buffered saline (PBS) solutions under a neutral or alkaline condition (pH 10.5) as used in formulation of decontaminants such as RSDL for skin decontamination. No evidence of oxime degradation was detectable in UPLC traces for at least 3 days as reported for similar oximes.<sup>20</sup>

## 3. Membrane Permeability In Vitro

Our design approach for dual-acting oximes was focused on hydrophobic augmentation in their scaffold domain for improved enzyme reactivation. However, we also wanted to retain their hydrophilicity enough for preventing adverse effects as seen with the relatively lipophilic DAM (clogP = 0.332), which are induced by its rapid distribution into lipid membranes and suppression of membrane-bound calcium channels.<sup>32, 33</sup> To evaluate such balanced properties, we compared predicted physicochemical properties as summarized in Table 1 that include calculated partition coefficient (*P*) between water and 1-octanol and calculated molar refractivity (CMR) as a measure of molecular volume. Compared to DAM (clogP = 0.332; CMR =

## ARTICLE

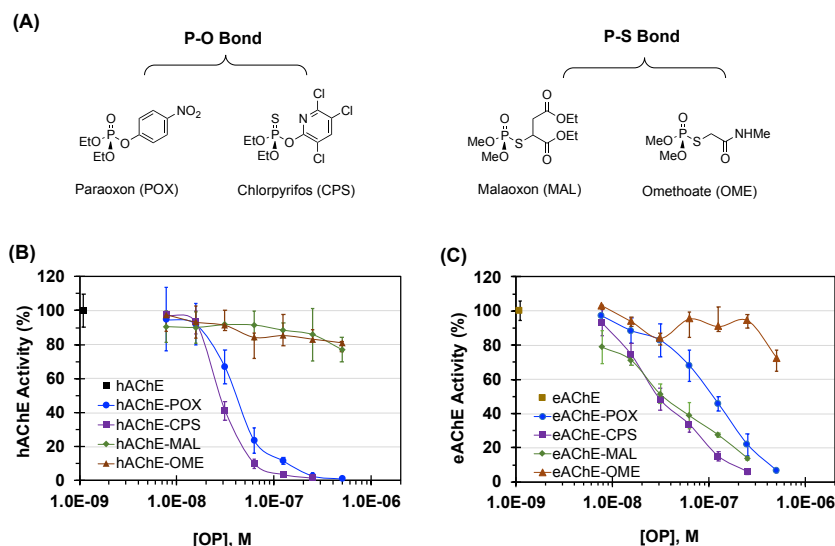


**Fig. 3** (A) Structures of four OPs tested that include paraoxon (POX), chlorpyrifos (CPS), malaoxon (MAL) and omethoate (OME). (B, C) Dose-dependent inhibition of human acetylcholinesterase (hAChE) and *Electrophorus electricus* acetylcholinesterase (eAChE) by OPs in PBS pH 8.0 at 23 °C *in vitro*. Each value represents a mean  $\pm$  standard deviation (SD,  $n = 3-6$ ).

2.72; charge = 0), oximes **1-9** each has a lower  $\text{clog}P$  value (except an outlier **4**), a higher CMR value and a positive charge (+1) due to its protonatable amine at physiological pH or quaternary ammonium cation (**4**). Each of these is favored for greater hydrophilicity by oximes than DAM.

In addition to physicochemical predictions, we determined the effective permeability ( $P_e$ ) of oximes in a parallel artificial membrane permeability assay (PAMPA) *in vitro*.<sup>39</sup> This assay measures the kinetics of compound distribution through synthetic lipid bilayers from a donor well to an acceptor well. Despite its simplicity, this assay provides  $P_e$  values which can be positively correlated with human skin permeability.<sup>39</sup> The permeability of compounds **1-9** was tested in PBS pH 7.4 at 23 °C, and the fraction of compound distribution into the acceptor well was quantified by UV-vis absorption traces as shown in Fig. S3 (ESI). Their  $P_e$  values were calculated according to an established equation<sup>39</sup> as summarized in Table 1. All oximes showed lower values of permeability relative to DAM (rel.  $P_e = 1.0$ ), which is consistent with their higher level of hydrophilicity suggested by predicted physicochemical properties. Three oximes **2, 3, 6** showed slight increases in permeability (rel.  $P_e = 0.27-0.38$ ) compared to **1** (rel.  $P_e = 0.23$ ). However, these data suggest that oxime compounds still remain relatively low in membrane permeability despite modifications at the scaffold domain.

#### 4. Reactivation of AChE-OP by Oxime

**AChE Inhibition.** Compound screening for enzyme reactivation was performed using two types of aqueous soluble AChE—human recombinant (hAChE) and *Electrophorus electricus* (eAChE)—and acetylthiocholine (ATCh) as their substrate in PBS pH 8.0 at 23 °C according to the Ellman's protocol.<sup>43</sup> Use of these enzymes in the assays of AChE reactivation has been already validated in literature.<sup>19, 20, 44-46</sup> Each enzyme was evaluated for its catalytic efficiency (0.2 U/mL) in terms of rate constant for substrate hydrolysis ( $k = \Delta A_{412 \text{ nm}}/\Delta t$ ;  $\text{min}^{-1}$ ) and relative enzyme activity (%) as summarized in Table S1 (ESI). hAChE and eAChE showed consistency in catalytic rate under their assay condition in which both enzyme types displayed up to  $1.2 \pm 0.28$  (accumulative  $n = 63$ )  $\times 10^{-1} \text{ min}^{-1}$  and  $1.1 \pm 0.013$  ( $n = 9$ )  $\times 10^{-1} \text{ min}^{-1}$  in  $k$  values, respectively, while their non-enzymatic (blank) control where AChE was absent showed relatively a lack of ATCh hydrolysis ( $k < \sim 1 \times 10^{-4} \text{ min}^{-1}$ ).

Four OP pesticides were tested here to verify their potencies in enzyme inhibition that include POX, chlorpyrifos (CPS), malaoxon (MAL) and omethoate (OME) as classified in Fig. 3A. Each of these has an either P-O or P-S bond that offers chemical reactivity<sup>47</sup> enough to serve as an OP surrogate to nerve agents and yet sufficient stability<sup>19, 20</sup> in aqueous media suited for AChE inactivation assays. Their dose-dependent potencies are presented in Fig. 3B and 3C with enzyme activity (%) plotted against OP concentration. In hAChE, POX and CPS showed potent inhibitions while MAL and OME each displayed only a weak inhibition. In eAChE, potent inhibitions were observed

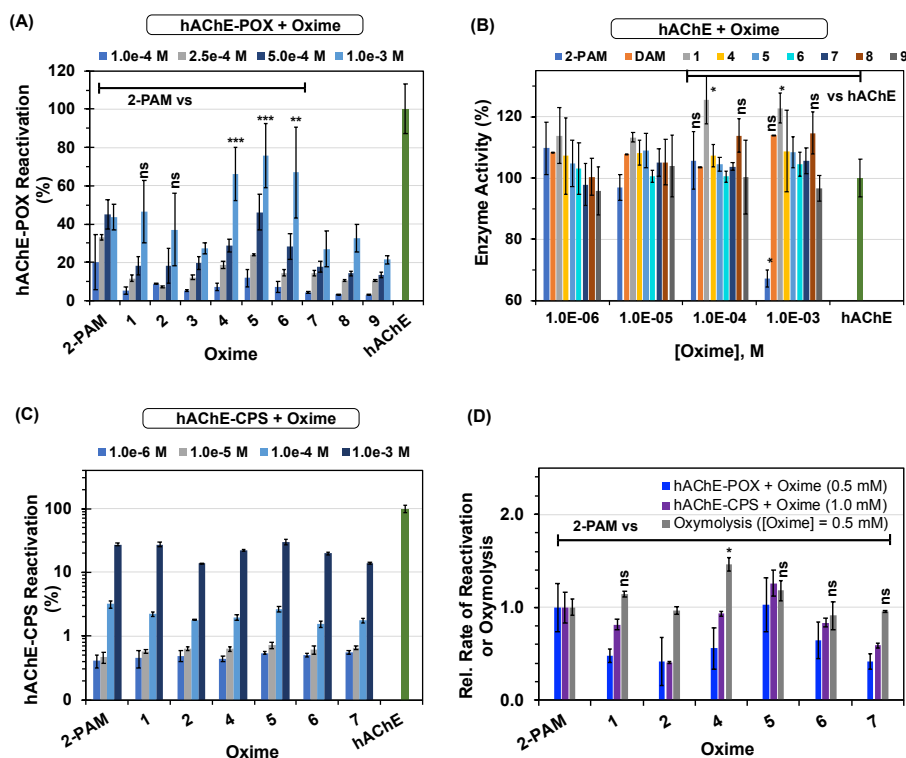


**Fig. 4** (A) Dose-dependent reactivation (%) of hAChE-POX (50 nM) by oximes 1–9. (B) The effect of oximes on hAChE activity (%) as a function of oxime concentration. (C) Dose-dependent reactivation (%) of hAChE-CPS (50 nM) by oximes. (D) Comparison of the rate ( $k = \Delta A_{412 \text{ nm}}/\Delta t$ ) of enzyme reactivation vs the rate of non-enzymatic oxymolysis by representative oximes relative to 2-PAM (rel. rate = 1.0). Each value represents a mean  $\pm$  SD ( $n = 3-6$ ). \*  $p$  value  $< 0.05$ . \*\*  $p < 0.01$ . \*\*\*  $p < 0.001$ . ns = no significance ( $p > 0.05$ ).

from all three OPs except OME which remained weakly inhibitory at its test range.  $IC_{50}$  (half-maximal inhibitory concentration) values were calculated from their inhibition curves by regression analysis as summarized in Table S1 (ESI). Our result in  $IC_{50}$  (POX = 18 nM, 51 nM; CPS = 8 nM, 18 nM; MAL = 21 nM, >600 nM; OME >600 nM) is in reasonable agreement with inhibitory potencies reported for POX (15 nM,<sup>48</sup> 50 nM<sup>20</sup>), CPS (30 nM,<sup>49</sup> 86 nM<sup>50</sup>) and relatively weak activity by MAL and OME.<sup>2</sup> Based on these results, only potent OP pesticides were selected for AChE inhibition in reactivation assays, in which the enzyme was treated with an OP at a concentration higher than its  $IC_{50}$  value.

**Reactivation of hAChE-OP.** Oxime compounds were screened to determine their abilities in the reactivation of OP-inhibited hAChE. Of two hAChE-OP types that were identified above, hAChE-POX served in the evaluation of the entire oxime library 1–9. In this screening, hAChE was pre-inhibited by POX ( $IC_{50} = 18$  nM) treatment at 50 nM for 30 min prior to the addition of test compounds at sub mM concentrations ( $10^{-4}$ – $10^{-3}$  M). Thus, this POX treatment led to complete loss of hAChE activity (<5%) prior to reactivation by test oximes. Their activities for enzyme reactivation are presented in relative activity (%) in Fig. 4A or equivalently in rate constant ( $k$ ;  $\Delta A_{412 \text{ nm}}/\Delta t$ ) values in Fig. S4 (ESI). As one of the standard reactivators,<sup>44, 51</sup> 2-PAM showed dose-dependent increases in enzyme activity with a maximal level of reactivation (45%) reached at 0.5 mM. All tested oximes showed lower

reactivation activities than 2-PAM at similar or lower concentrations. However, 5 was able to produce a similar activity at 0.5 mM. In addition, 4–6 were more effective at 1.0 mM with 66–76% than 2-PAM ( $p < 0.01$ – $0.001$ ) while 1, 2 showed no significant differences to 2-PAM.

Among the oximes, most remarkable activities are evident with an *N*-ethyl (4), *N*-pyrrolidinyl (5) and *N*-methyl (6) modification given their higher activities at most test concentrations ( $p$  value  $< 0.05$ – $0.01$ ). However, despite its tertiary or quaternary *N*-methylation, 2, 3 failed to improve its activity relative to 1. These results serve as evidence supportive of *N*-alkyl selectivity and the importance of spacer length. Heterocycle and hydrophilic comparators 7–9 exhibited either comparable or overall lower activities, which is not surprising given their unfavorable scaffold modifications.

In addition to enzyme reactivation, oximes were evaluated for their effect on hAChE activity compared to 2-PAM which shows a reversible enzyme inhibition in the millimolar range.<sup>42</sup> Fig. 4B summarizes hAChE activities measured after treatment with representative oximes. 2-PAM showed a significant decrease to 67% at 1.0 mM, which is consistent with earlier reports.<sup>19, 20</sup> However, hAChE treated with oximes except 1 retained the enzyme activity as effective as untreated hAChE. Interestingly, the treatment with 1 otherwise increased the activity by up to 25% at 0.1–1.0 mM. We examined whether this is attributable to an increase in the rate of oxymolysis, which refers to the hydrolysis of ATCh (0.25 mM) catalyzed by oxime without hAChE added. Relative rates of oxymolysis presented in



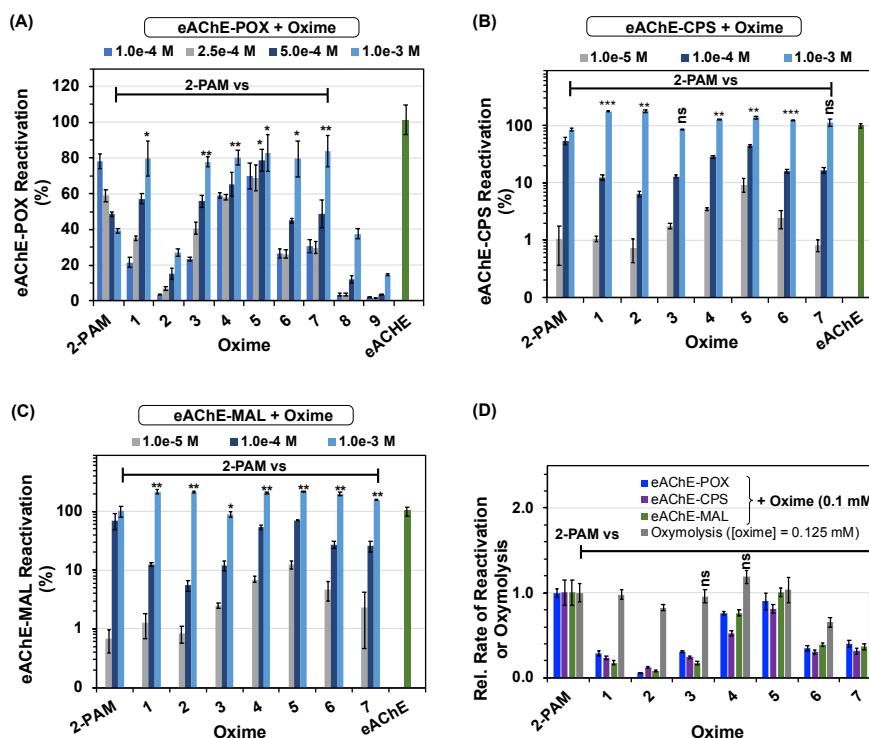


**Fig. 5** (A–C) Dose-dependent reactivation (%) of eAChE-POX (500 nM), eAChE-CPS (50 nM) and eAChE-MAL (250 nM) by oximes 1–9. (D) Relative rate ( $k = \Delta A_{412\text{ nm}}/\Delta t$ ) of eAChE-OP reactivation and non-enzymatic oxymolysis by representative oximes. Each value represents a mean  $\pm$  SD ( $n = 3-6$ ). \*  $p$  value  $< 0.05$ . \*\*  $p < 0.01$ . \*\*\*  $p < 0.001$ . ns = no significance ( $p > 0.05$ ).

Fig. 4D indicate non-significant differences among tested oximes and thus no positive correlation between the enzyme reactivation and the non-enzymatic oxymolysis. Therefore, variations in enzyme activity could be better accounted for by modifications in the scaffold domain rather than the oxime core which is more responsible for oxymolysis.

Following their primary screening above, selected oximes were further evaluated against hAChE inactivated by CPS (50 nM) as presented in Fig. 4C. In general, it was harder to reactivate hAChE-CPS than hAChE-POX at 0.1 mM or lower oxime concentrations where only 2–3% of enzyme activity could be restored. At the highest dose (1.0 mM), reactivation occurred to a greater extent by 2-PAM (27%) and oximes (14–30%), suggesting their potential for a broad spectrum of enzyme reactivation. In summary, nine compounds were evaluated for enzyme reactivation against two types of hAChE-OP, and 4–6 were identified as promising reactivators given their significant activities comparable to 2-PAM.

**Reactivation of eAChE-OP.** Compound screening for enzyme reactivation was expanded to electric eel AChE. Thus, eAChE pre-inhibited by POX (500 nM) was treated with oximes 1–9 at sub mM concentrations and their reactivation activities were determined as presented in Fig. 5A and Fig. S6 (ESI) for rate constant values ( $k$ ;  $\text{min}^{-1}$ ). 2-PAM showed a maximal activity of 78% at 0.1 mM, which however gradually decreased at higher concentrations. This reversed concentration dependency, as noted in earlier works,<sup>52,53</sup> could be attributable to its ability for competitive enzyme inhibition as evident in Fig. 4B.

Like in hAChE-POX reactivation, 2 failed to show improved activities compared to 1 although its *N*-methyl quaternary compound 3 was able to restore reactivation activities as effective as 1. A majority of compounds 3–7 showed significant activities with 21–70% at 0.1 mM which grew higher in a concentration-dependent manner (Fig. 5A). Of particular note are 4 and 5, each more effective than 1 at most concentrations while 3, 6, 7 exhibited comparable or slightly lower activities. Nonetheless, each of these oximes was still more effective than 2-PAM with 80–84% of enzyme activity restored at 1.0 mM. Comparators 8 and 9 showed overall lower activities than 1 as observed in hAChE-POX reactivation.

Screening of oximes 1–7 was also performed against eAChE pre-inactivated by CPS (50 nM) or MAL (250 nM) as presented in Fig. 5B and 5C. These plots show similarities in concentration-activity trends between eAChE-CPS and eAChE-MAL. Thus, in general, 2 displayed overall lower activities than 1 while its quaternary analog 3 exhibited improved activities. It is notable that despite being less active than 2-PAM at 0.1 mM, all oximes turned out to be more active at 1.0 mM where the enzyme was fully and more effectively reactivated. The plot of oxymolysis compared at 0.125 mM (Fig. 5D) indicates no positive correlation with reactivation activity. In summary, oxime screening performed with three types of eAChE-OP led to identification of compounds 4–7 that displayed promising reactivation activities. These compounds demonstrated significant activities in the reactivation of hAChE-OP as well.

In summary, a 9-member oxime library was prepared and thoroughly investigated for reactivation activities against

## ARTICLE

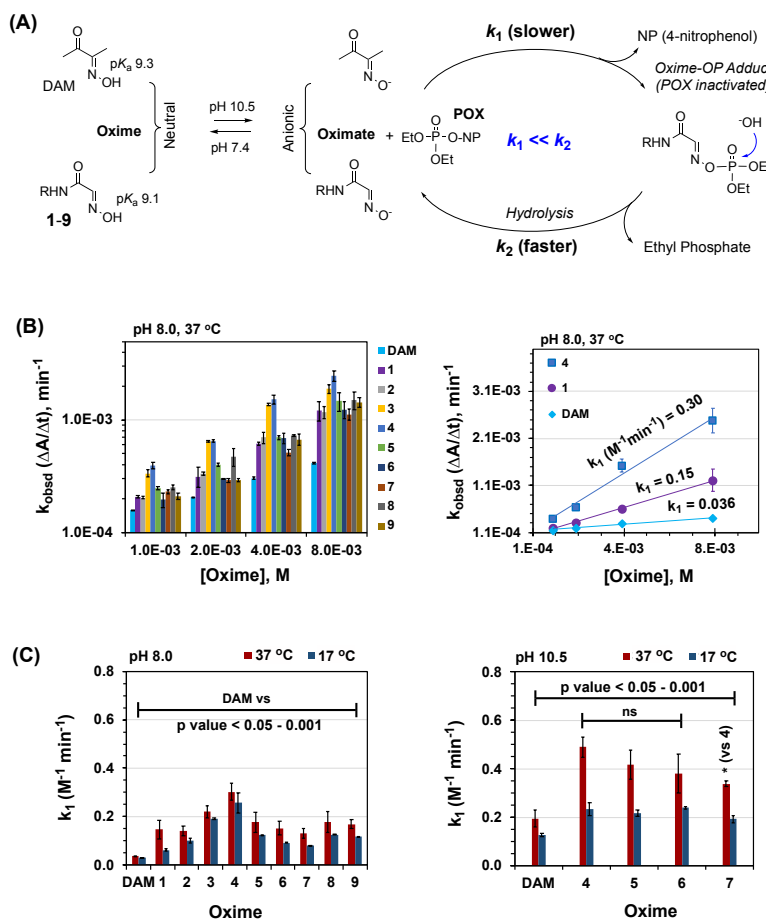


**Fig. 6** (A) Kinetic parameters of POX inactivation via nucleophilic oxime catalysis. Rate =  $-d[\text{POX}]/dt = k_1[\text{POX}][\text{Oxime}]$ . (B) Plots of observed rate constant ( $k_{\text{obsd}}$ ;  $\text{min}^{-1}$ ) against oxime concentration in PBS pH 8.0 at 37 °C.  $[\text{POX}]_{\text{fixed}} = 30 \mu\text{M}$ . Inset (right): Illustration of  $k_1$  values calculated through linear regression analysis under a pseudo first-order condition ( $k_1[\text{Oxime}] = k_{\text{obsd}}$ ). (C) Plots of  $k_1$  values determined at pH 8.0 (left) or pH 10.5 (right), each at  $17 \pm 2$  and  $37 \pm 1$  °C. Data points are mean  $\pm$  SD ( $n = 3$ ). \*  $p$  value  $< 0.05$ . ns = no significance

hAChE-OP and eAChE-OP, each inactivated by POX, CPS or MAL. Significant enhancements in enzyme activity were observed from compounds with hydrophobic modifications with *N*-ethyl (4), *N*-pyrrolidinyl (5) and *N*-methyl (6). These were able to reactivate the enzymes with good potencies comparable to 2-PAM and with a broad spectrum of activity against both enzyme subtypes and all three OPs. This result is in line with high sequence homologies in the catalytic pocket of AChE<sup>54</sup> and the presence of identical or similar alkyl groups introduced after OP phosphorylation such as methyl (MAL) or ethyl (POX, CPS). In contrast, lower activities were observed from comparators modified with polar moieties (8, 9). These results enabled us to establish a structure-activity relationship in the scaffold domain by which our design concept could be validated. We anticipate that these experimental results can be better definable by employing computational approaches such as X-ray crystal

structure-based modelling and docking studies,<sup>46, 55</sup> which constitutes a follow-up study.

## 5. Oxime Screening for POX Inactivation

**Rate Constants.** Following enzyme assays, we focused on oxime reactivity in the chemical inactivation of OP. The mechanism of OP inactivation occurs through nucleophilic catalysis as illustrated with POX in Fig. 6A.<sup>19, 20</sup> In the first step, the oxime molecule, which exists as either a neutral oxime or a deprotonated oximate, attacks POX and forms a neutralized adduct with the release of 4-nitrophenol (4-NP) (bimolecular rate constant  $k_1$ ). In the second step, the inactivated adduct undergoes fragmentations via Beckmann rearrangement (not shown)<sup>35, 56</sup> and hydrolytic cleavage to diethyl phosphate (rate



ARTICLE

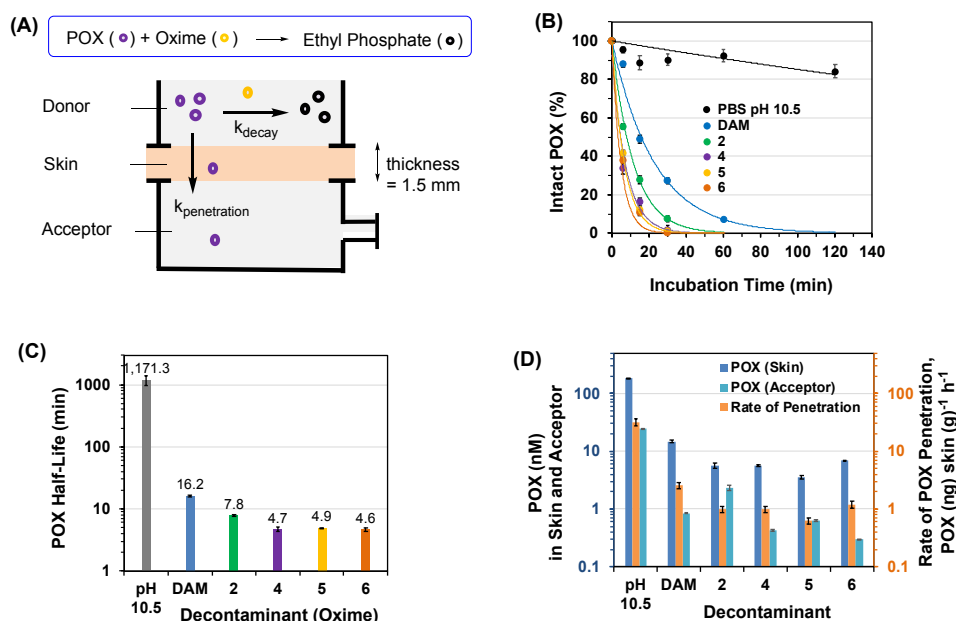


**Fig. 7** Efficacy of POX decontamination from porcine skin at 37 °C *in vitro* by treatment with oximes. (A) A diagram depicting a Franz cell setup employed in decontamination experiments. (B, C) Decay curves (% area under curve) and half-life ( $t_{1/2}$ ) values of POX in the donor compartment after oxime treatment. (D) Concentration of POX detected in the skin extract and acceptor compartment, and its rate of penetration into the skin layer. Each value represents a mean  $\pm$  SD in detection ( $n = 2$ ).

constant  $k_2$ ), completing a catalytic cycle in OP inactivation. The first step occurs much more slowly than the second step ( $k_2/k_1 \geq 100\text{--}1000$ ),<sup>47, 57</sup> and thus its rate ( $k_1$ ) determines the overall rate of POX inactivation as measured in this study.

**POX Inactivation.** The chemical reactivity of oximes for OP inactivation was measured using POX as a model OP surrogate.<sup>35, 47</sup> Their reactivities are quantifiable by the values of  $k_{obsd}$ , the observed rate constant determined at a particular oxime concentration, and generally, by the values of  $k_1$  which is derived from  $k_{obsd}$  values. Both of these kinetic parameters were determined in a chemical assay in which a fixed amount of POX (30  $\mu\text{M}$ ) reacted with oxime 1–9 added in a large molar excess ( $[\text{Oxime}]_{\text{variable}} = 0.5\text{--}8.0 \text{ mM}$ ) in a 96-well microplate for high-throughput screening.<sup>19, 20</sup> Time courses of POX inactivation, which occurred under various pH (8.0, 10.5) and temperature (17, 37 °C) conditions, are presented by plotting  $A_{400 \text{ nm}}$  against reaction time as compiled in Fig. S7–S9 (ESI). These curves were analyzed to extract  $k_{obsd}$  values by linear regression analysis (slope =  $\Delta A_{400 \text{ nm}}/\Delta t$ ) (Fig. S10, SI).

Fig. 6B shows a representative set of  $k_{obsd}$  values acquired at pH 8.0, 37 °C, the same condition as in enzyme reactivation. This figure (inset, right) illustrates how  $k_1$  values are calculated for DAM, 1 and 4 by linear regression analysis of  $k_{obsd}$  vs oxime concentration under a pseudo-first order assumption (rate =

$k_1[\text{POX}][\text{Oxime}] \approx k_{obsd}[\text{POX}]$  where  $[\text{Oxime}] \gg [\text{POX}]$ ).<sup>57</sup> It shows higher  $k_{obsd}$  values (more reactive) by oximes than DAM. In particular, most remarkable reactivities were observed with 3 and 4, each modified with *N*-methyl or *N*-ethyl moieties.

Fig. 6C (left) shows  $k_1$  values for oximes 1–9 determined at pH 8.0 at either 17 or 37 °C. These values confirm ~4 to 8-fold higher reactivities of oximes than DAM. In addition, most oximes including 3 and 4 show greater reactivities than 1 by a factor of up to 2 (37 °C) or 4 (17 °C). Their  $k_1$  values are generally higher at 37 °C than 17 °C, which is accordingly indicative of shorter POX half-life ( $t_{1/2} = \log(2)/k$ ) at a higher temperature. This dependency on temperature is consistent with the endothermic nature of the reaction of POX inactivation.<sup>19, 20</sup>

We also measured  $k_1$  values at an elevated pH 10.5 where due to an increased oxime acidity ( $pK_a = 9.1$ ), POX inactivation occurs predominantly by an oximate species (fraction > 0.95)<sup>20</sup> which is known to be more reactive than its neutral oxime (Fig. 6A).<sup>20</sup> Values of  $k_1$  determined for selected oximes 4–7 show an increase in rate up to 5.4 (DAM) or 2.6-fold at 37 °C than those acquired at pH 8.0 (Fig. 6C, right). This result is in agreement with faster OP inactivation at higher pH conditions in earlier works.<sup>19, 20</sup> Temperature dependency remained applicable at pH 10.5 in which  $k_1$  values increased by a factor of 1.5–2.1 as the medium temperature was elevated from 17 °C to 37 °C.

In summary, POX inactivation assays showed that all tested oximes are comparable to or more reactive than the unmodified oxime **1**. They showed more effective catalysis up to 2 or 4-fold under an identical condition. Their rates varied with reaction conditions such that faster POX inactivation occurred at more alkaline pH (pH 10.5 > pH 8.0) and higher temperature (37 °C > 17 °C). This suggests the importance of applying an oxime decontaminant under an optimal condition as performed here. In addition, unlike in AChE reactivation assays, we have not seen any loss of reactivity by scaffold modifications. This suggests a lack of any negative impact on oxime nucleophilicity by steric interference that might arise from scaffold modifications.

## 6. Skin Decontamination *In Vitro*

Following identification of oxime leads in enzyme reactivation and chemical OP inactivation, representative oximes **2**, **4–6** were investigated for their efficacy in POX decontamination on intact porcine skin. This assay was performed in a Franz cell setup as reported<sup>19, 20, 30</sup> where a patch of dehaired porcine skin (thickness = 1.5 mm) was clamped as the test tissue between the donor and acceptor compartment (Fig. 7A). After 2 minutes of POX addition (50 μM) in the donor side, the exposed skin surface was treated with 0.3 M DAM (RSDL) or oxime, each formulated in PBS pH 10.5, or the PBS vehicle alone (pH 10.5).

First, the decay kinetics of POX which occurred in the donor compartment was established by UPLC analysis of POX concentrations over incubation time (Fig. 7B). As anticipated, POX decay occurred rapidly after the treatment with DAM or each oxime but not with PBS pH 10.5 in which POX remained almost stable. POX half-life values were calculated from the decay curves as plotted in Fig. 7C. Treatments with **4–6** enabled faster POX decays ( $t_{1/2}$  = 4.6–4.9 min) than **2** ( $t_{1/2}$  = 7.8 min), DAM ( $t_{1/2}$  = 16.2 min) or the PBS vehicle ( $t_{1/2}$  = 1171 ± 215 min). Their superior efficiency in skin decontamination is consistent with their higher  $k_1$  values of POX inactivation determined in solution kinetics, which are predictive of faster POX inactivation (Fig. 6B).

Second, we determined the level of POX penetration into the skin layer and subsequently flow through the acceptor side. The amount of POX in each analyte was quantified by LC mass spectrometry analysis of the skin harvested after 2 h treatment and the aliquot from the acceptor compartment (Fig. 7D). The highest level of POX was detected in the skin treated with the PBS vehicle (183 nM). This is 12 to 50-fold larger than the level detected in the skin treated with DAM or oximes. Similarly, the POX level was highest in the acceptor aliquot after the PBS treatment. The efficiency of POX decontamination is further corroborated with the rate of penetration, which is defined here as the amount of POX (ng) that penetrates into one gram of skin tissue per hour. As shown in Fig. 7D, oximes **4–6** (rate = 0.62–1.2, unit = POX (ng)/[skin (g) × h]) show lower rates of POX penetration than DAM (2.6) or PBS (32).

In summary, lead oximes displayed superb efficacy in the skin decontamination of POX *in vitro*. Like RSDL which is formulated with DAM at pH >10.8, representative oximes were formulated at pH 10.5 and tested to demonstrate their efficacy

in POX decontamination on porcine skin *in vitro*. Compounds **4–6** were more effective in blocking POX penetration into skin by a factor of 2 to 4 than DAM. Overall, these results suggest a positive correlation between chemical reactivity in solution kinetics and skin decontamination efficacy.

## Experimental

**Synthesis of Oximes 1–9.** Oxime **1** was prepared according to the method A reported in our earlier work (Scheme 1).<sup>20</sup> All other oximes **2–9** were synthesized by either method A or B by reacting ethyl 2-(hydroxyimino)acetate<sup>20</sup> with a requisite amine (3 molar equiv) at 45 °C. Details of their synthetic methods and characterizations are described in ESI.

**Parallel Artificial Membrane Permeability Assay (PAMPA).** The permeability assay was performed at 23 °C using a PAMPA kit (PION, Inc.) as described in SI. Permeability rate ( $P_e$ , cm s<sup>-1</sup>) was calculated as defined in literature.<sup>39, 58</sup>

**AChE Assay.** This assay employed two types of soluble AChE that include *Electrophorus electricus* AChE (eAChE) and human recombinant AChE (hAChE), both purchased from Sigma-Aldrich. It was performed according to the Ellman's protocol<sup>43</sup> using acetylthiocholine (ATCh) as its substrate in PBS pH 8.0 at 23 °C as described in SI according to our earlier works.<sup>19, 20</sup> The rate constant  $k$  for enzyme kinetics was obtained by plotting  $A_{412\text{ nm}}$  against time (min) and calculating its slope ( $\Delta A_{412\text{ nm}}/\Delta t$ ; min<sup>-1</sup>) at an early linear phase (0–15 min). Efficiency (%) of enzyme reactivation was calculated from rate constants ( $k$ ) as reported in literature.<sup>15, 19, 20, 43, 59</sup>

AChE inhibition by OP was performed by treating AChE (0.2 U/mL) with OP (POX, CPS, MAL, OME) in a range of concentrations (10<sup>-9</sup> – 10<sup>-6</sup> M). Stock solutions for OPs were prepared each at 1.0 mM in DMSO and diluted with PBS pH 8.0 10<sup>3</sup> to 10<sup>6</sup>-fold to their test concentrations. IC<sub>50</sub> values for each OP were estimated from its dose-enzyme activity (%) curves through a linear or non-linear regression analysis. For enzyme reactivation, AChE (0.2 U/mL) was pre-inhibited to less than 5% of its original activity by treatment with OP prior to treatment with a test oxime compound in a variable range of concentrations (10<sup>-5</sup>–10<sup>-3</sup> M).

**Screening of Chemical Reactivity in POX Inactivation.** Reaction kinetics for POX (30 μM in PBS 8.0 containing 0.3% DMSO) inactivation by oxime was performed by spectrometric analysis as reported previously.<sup>19, 20, 29</sup> Its reaction progress was monitored by focusing on time-dependent growth in absorbance by its byproduct 4-NP at 400 nm ( $\lambda_{\text{max}}$ ) as described in SI. Data were processed and analyzed for determining rate constants ( $k_{\text{obsd}}$ ,  $k_1$ ) as described in earlier works.<sup>19, 20, 29</sup>

**Skin Decontamination *In Vitro*.** Topical decontamination of POX by oxime was performed following the protocol described in our earlier works.<sup>19, 20, 30</sup> Porcine skin was purchased in a dehaired form (1.5 mm thick) from Stellen Medical and used as received. According to the supplier, its dehairing was performed simply

by shaving the skin as much as possible. It was clamped as a test tissue between the donor and acceptor compartment in a Franz cell device controlled at 37 °C (Fig. 7A). The donor side was loaded with POX (50 μM, 0.4 mL) in PBS pH 10.5 containing 0.5% DMSO and incubated for 2 min prior to loading a decontaminant (0.3 M, 0.4 mL) formulated in PBS pH 10.5. The device kept for 2 h while analyte solutions were periodically aliquoted from the donor side as specified in Fig. 7. After the 2 h treatment, the skin tissue was recovered and treated with 100% EtOH (1.0 mL) to extract POX penetrated. In addition, an analyte was aliquoted from the acceptor side at the end of the experiment ( $t = 2$  h). Analyte samples were analyzed for POX amounts by either UPLC or LC mass spectrometry (LCMS) following the methods developed earlier.<sup>19, 20, 30</sup> The rate of skin penetration is arbitrarily defined here as the amount of POX (ng) detected per tissue weight (g) per treatment time (h): (unit = POX ng × (skin tissue g × h)<sup>-1</sup>).

**Statistical Analysis.** Statistical analyses were performed by a Student's paired t-Test with a two tailed distribution. Differences with  $p$  values of less than 0.05 are considered as statistically significant.

**Hazardous Materials.** Caution: OP chemicals (paraoxon, chlorpyrifos, malaoxon and omethoate) are generically hazardous and should be handled carefully.

## Conclusions

This article described a new approach in the structure-guided<sup>45, 46, 55</sup> or fragment-based<sup>60-62</sup> methodologies developed to address current challenges and limitations in the design of effective therapeutics. It tested a concept of dual acting oximes with a focus on therapeutic OP decontamination that occurs through OP inactivation (scavenging) and AChE reactivation. Their design concept involved tethering a common core of OP-reactive oxime to a variable amine-functionalized scaffold for optimal enzyme reactivation. This structural integration also allowed retention of beneficial physicochemical properties such as low membrane permeability ( $P_e$ ) which can play a critical role in preventing rapid membrane distribution associated with lipophilic DAM.<sup>32</sup> In summary, this study tested a new design principle for dual-acting oximes toward the development of OP decontaminants and identified a few leads on the basis of a unique set of data distinct from earlier studies<sup>16, 42, 46</sup> of identical or comparable oximes.

This study offers new insights in the development of therapeutic decontaminants for OP exposure. Small oximes such as DAM<sup>18</sup> have been demonstrated for their efficient scavenging of OP. However, despite their applications in skin decontamination, their efficacy is limited due to a lack of primary antidote activities such as AChE reactivation. In this study, we addressed such unmet needs by identifying dual acting oximes that are able to engage in not only OP scavenging but also AChE reactivation in OP-exposed tissues. This class of oximes have potential to serve as a new generation of therapeutic agents in the treatment of OP exposure. This aspect

of their practical applications is anticipated to constitute a subject of future studies.

## Author Contributions

Each author made significant contributions: JC & ST (methodology, investigation, formal analysis), KY & RH (investigation, formal analysis), and SKC (funding acquisition, conceptualization and writing). All authors have given approval to the final version of the manuscript.

## Conflicts of interest

The authors declare no competing financial interest.

## Acknowledgements

This work was supported by the US Defense Threats Reduction Agency–DOD [HDTRA1-17-C-00001].

## References

- 1 J. A. Vale, *Toxicology*, 2007, **240**, 141–142.
- 2 F. Worek, H. Thiermann and T. Wille, *Arch. Toxicol.*, 2020, **94**, 2275–2292.
- 3 G. Mercey, T. Verdet, J. Renou, M. Kliachyna, R. Baati, F. Nachon, L. Jean and P.-Y. Renard, *Acc. Chem. Res.*, 2012, **45**, 756–766.
- 4 H. W. Chambers and J. E. Chambers, *Pestic. Biochem. Physiol.*, 1989, **33**, 125–131.
- 5 V. S. Lin, R. F. Volk, A. J. DeLeon, L. N. Anderson, S. O. Purvine, A. K. Shukla, H. C. Bernstein, J. N. Smith and A. T. Wright, *Chem. Res. Toxicol.*, 2020, **33**, 414–425.
- 6 L. M. Schopfer, T. Voelker, C. F. Bartels, C. M. Thompson and O. Lockridge, *Chem. Res. Toxicol.*, 2005, **18**, 747–754.
- 7 M. C. Franklin, M. J. Rudolph, C. Ginter, M. S. Cassidy and J. Cheung, *Proteins: Struct., Funct., Bioinf.*, 2016, **84**, 1246–1256.
- 8 J. Mukherjee, P. T. Wong, S. Tang, K. Gam, A. Coulter, J. R. Baker and S. K. Choi, *Mol. Pharmaceutics*, 2015, **12**, 4498–4508.
- 9 J. H. Wills, *J. Med. Chem.*, 1961, **3**, 353–359.
- 10 I. N. Somin and S. G. Kuznetsov, *Pharm. Chem. J.*, 1968, **2**, 449–453.
- 11 P. Eyer, *Toxicol. Rev.*, 2003, **22**, 165–190.
- 12 D. Jovanović, *Arch. Toxicol.*, 1989, **63**, 416–418.
- 13 T. N. Pashirova, A. Braïki, I. V. Zueva, K. A. Petrov, V. M. Babaev, E. A. Buriilova, D. A. Samarkina, I. K. Rizvanov, E. B. Souto, L. Jean, P.-Y. Renard, P. Masson, L. Y. Zakharova and O. G. Sinyashin, *J. Controlled Release*, 2018, **290**, 102–111.
- 14 J. C. DeMar, E. D. Clarkson, R. H. Ratcliffe, A. J. Campbell, S. G. Thangavelu, C. A. Herdman, H. Leader, S. M. Schulz, E. Marek, M. A. Medynets, T. C. Ku, S. A. Evans, F. A. Khan, R. R. Owens, M. P. Nambiar and R. K. Gordon, *Chem.-Biol. Interact.*, 2010, **187**, 191–198.
- 15 G. E. Garcia, A. J. Campbell, J. Olson, D. Moorad-Doctor and V. I. Morthole, *Chem.-Biol. Interact.*, 2010, **187**, 199–206.
- 16 Z. Radić, R. K. Sit, Z. Kovarik, S. Berend, E. Garcia, L. Zhang, G. Amitai, C. Green, B. Radić, V. V. Fokin, K. B. Sharpless and P. Taylor, *J. Biol. Chem.*, 2012, **287**, 11798–11809.
- 17 Q. Zhuang, A. J. Franjesevic, T. S. Corrigan, W. H. Coldren, R. Dicken, S. Sillart, A. DeYong, N. Yoshino, J. Smith, S. Fabry, K. Fitzpatrick, T. G. Blanton, J. Joseph, R. J. Yoder, C. A. McElroy, Ö. D. Ekici, C. S. Callam and C. M. Hadad, *J. Med. Chem.*, 2018, **61**, 7034–7042.
- 18 E. H. Braue, K. H. Smith, B. F. Doxzon, H. L. Lumpkin and E. D. Clarkson, *Cutaneous Ocul. Toxicol.*, 2011, **30**, 15–28.
- 19 P. Wong, S. Bhattacharjee, J. Cannon, S. Tang, K. Yang, S. Bowden, V.

- Varnau, J. J. O'Konek and S. K. Choi, *Org. Biomol. Chem.*, 2019, **17**, 3951–3963.
- 20 S. Tang, P. T. Wong, J. Cannon, K. Yang, S. Bowden, S. Bhattacharjee, J. J. O'Konek and S. K. Choi, *Chem.-Biol. Interact.*, 2019, **297**, 67–79.
- 21 F. Terrier, P. Rodriguez-Dafonte, E. Le Guevel and G. Moutiers, *Org. Biomol. Chem.*, 2006, **4**, 4352–4363.
- 22 O. Cohen, C. Kronman, L. Raveh, O. Mazor, A. Ordentlich and A. Shafferman, *Mol. Pharmacol.*, 2006, **70**, 1121–1131.
- 23 D. E. Lenz, E. D. Clarkson, S. M. Schulz and D. M. Cerasoli, *Chem.-Biol. Interact.*, 2010, **187**, 249–252.
- 24 S. K. Choi, *Nanomaterials*, 2021, **11**, 224.
- 25 C. M. Hartshorn, A. Singh and E. L. Chang, *J. Mater. Chem.*, 2002, **12**, 602–605.
- 26 R. K. Totten, M. H. Weston, J. K. Park, O. K. Farha, J. T. Hupp and S. T. Nguyen, *ACS Catal.*, 2013, **3**, 1454–1459.
- 27 D. B. Dwyer, D. T. Lee, S. Boyer, W. E. Bernier, G. N. Parsons and W. E. Jones, *ACS Appl. Mater. Interfaces*, 2018, **10**, 25794–25803.
- 28 P. Li, S.-Y. Moon, M. A. Guelta, L. Lin, D. A. Gómez-Gualdrón, R. Q. Snurr, S. P. Harvey, J. T. Hupp and O. K. Farha, *ACS Nano*, 2016, **10**, 9174–9182.
- 29 S. Bharathi, P. T. Wong, A. Desai, O. Lykhytska, V. Choe, H. Kim, T. P. Thomas, J. R. Baker and S. K. Choi, *J. Mater. Chem. B*, 2014, **2**, 1068–1078.
- 30 P. T. Wong, S. Tang, J. Cannon, K. Yang, R. Harrison, M. Ruge, J. J. O'Konek and S. K. Choi, *ACS Appl. Mater. Interfaces*, 2020, **12**, 33500–33515.
- 31 J. Misik, R. Pavlikova, D. Josse, J. Cabal and K. Kuca, *Toxicol. Mech. Methods*, 2012, **22**, 520–525.
- 32 M. W. Fryer, P. W. Gage, I. R. Neering, A. F. Dulhunty and G. D. Lamh, *Pflugers Arch - Eur J Physiol*, 1988, **411**, 76–79.
- 33 G. J. Huang and J. J. McArdle, *J. Physiol. (Oxford, U. K.)*, 1992, **447**, 257–274.
- 34 T. J. Walters, D. S. Kauvar, J. Reeder and D. G. Baer, *Mil. Med.*, 2007, **172**, 318–321.
- 35 M. Fentabil, M. Gebremedhin, J. G. Purdon, L. Cochrane and V. S. Goldman, *Toxicol. Lett.*, 2018, **293**, 241–248.
- 36 M. V. Rajapurkar, G. B. Koelle and P. Smart, *J. Pharmacol. Exp. Ther.*, 1958, **123**, 247–253.
- 37 J. W. Skovira, J. C. O'Donnell, I. Koplovitz, R. K. Kan, J. H. McDonough and T.-M. Shih, *Chem.-Biol. Interact.*, 2010, **187**, 318–324.
- 38 J. C. Ma and D. A. Dougherty, *Chem. Rev. (Washington, DC, U. S.)*, 1997, **97**, 1303–1324.
- 39 G. Ottaviani, S. Martel and P.-A. Carrupt, *J. Med. Chem.*, 2006, **49**, 3948–3954.
- 40 H.-P. Lau and C. D. Gutsche, *J. Am. Chem. Soc.*, 1978, **100**, 1857–1865.
- 41 D. Gündisch, M. Andrä, L. Munoz and M. Cristina Tilotta, *Bioorg. Med. Chem.*, 2004, **12**, 4953–4962.
- 42 R. K. Sit, Z. Radić, V. Gerardi, L. Zhang, E. Garcia, M. Katalinić, G. Amitai, Z. Kovarik, V. V. Fokin, K. B. Sharpless and P. Taylor, *J. Biol. Chem.*, 2011, **286**, 19422–19430.
- 43 G. L. Ellman, K. D. Courtney, V. Andres jr and R. M. Featherstone, *Biochem. Pharmacol. (Amsterdam, Neth.)*, 1961, **7**, 88–95.
- 44 F. Worek, H. Thiermann, L. Szinicz and P. Eyer, *Biochem. Pharmacol. (Amsterdam, Neth.)*, 2004, **68**, 2237–2248.
- 45 A. J. Franjesevic, S. B. Sillart, J. M. Beck, S. Vyas, C. S. Callam and C. M. Hadad, *Chem. - Eur. J.*, 2019, **25**, 5337–5371.
- 46 L. Gorecki, O. Gerlits, X. Kong, X. Cheng, D. K. Blumenthal, P. Taylor, C. Ballatore, A. Kovalevsky and Z. Radić, *J. Biol. Chem.*, 2020, **295**, 4079–4092.
- 47 E. J. Behrman, M. J. Biallas, H. J. Brass, J. O. Edwards and M. Isaks, *J. Org. Chem.*, 1970, **35**, 3069–3075.
- 48 D. E. Lorke and G. A. Petroianu, *J. Appl. Toxicol.*, 2019, **39**, 101–116.
- 49 C. R. D. Assis, A. G. Linhares, V. M. Oliveira, R. C. P. França, E. V. M. M. Carvalho, R. S. Bezerra and L. B. de Carvalho, *Sci. Total Environ.*, 2012, **441**, 141–150.
- 50 A. Topal, M. Şişecioğlu, M. Atamanalp, A. Işık and B. Yılmaz, *J. Appl. Anim. Res.*, 2016, **44**, 243–247.
- 51 F. Worek, G. Reiter, P. Eyer and L. Szinicz, *Arch. Toxicol.*, 2002, **76**, 523–529.
- 52 D. Jun, L. Musilova, K. Musilek and K. Kuca, *Int. J. Mol. Sci.*, 2011, **12**, 2077–2087.
- 53 G. A. Petroianu, K. Arafat, S. M. Nurulain, K. Kuća and J. Kassa, *J. Appl. Toxicol.*, 2007, **27**, 168–175.
- 54 H. Dvir, I. Silman, M. Harel, T. L. Rosenberry and J. L. Sussman, *Chemico-Biological Interactions*, 2010, **187**, 10–22.
- 55 G. Santoni, J. de Sousa, E. de la Mora, J. Dias, L. Jean, J. L. Sussman, I. Silman, P.-Y. Renard, R. C. D. Brown, M. Weik, R. Baati and F. Nachon, *J. Med. Chem.*, 2018, **61**, 7630–7639.
- 56 C. A. Boulet and A. S. Hansen, *Phosphorus, Sulfur, and Silicon and the Related Elements*, 1991, **57**, 147–161.
- 57 J. C. Lamb, G. M. Steinberg, S. Solomon and B. E. Hackley, *Biochemistry*, 1965, **4**, 2475–2484.
- 58 H. Yu, Q. Wang, Y. Sun, M. Shen, H. Li and Y. Duan, *PLOS ONE*, 2015, **10**, e0116502.
- 59 M. C. de Koning, G. Horn, F. Worek and M. van Grol, *Eur. J. Med. Chem.*, 2018, **157**, 151–160.
- 60 G. Wu, Y. Gao, D. Kang, B. Huang, Z. Huo, H. Liu, V. Poongavanam, P. Zhan and X. Liu, *MedChemComm*, 2018, **9**, 149–159.
- 61 Z. Zhang, Y. Wang, Y. Zhang, J. Li, W. Huang and L. Wang, *MedChemComm*, 2019, **10**, 1180–1186.
- 62 X.-B. Wang, F.-C. Yin, M. Huang, N. Jiang, J.-S. Lan and L.-Y. Kong, *RSC Med. Chem.*, 2020, **11**, 225–233.